

## PULSE SHARPENING BY MAGNETIC COMPRESSION\*

George A. Mundy

*Stanford Linear Accelerator Center,  
Stanford University, Stanford, CA 94309*

### Abstract

The design and performance of a ferrite-loaded pulse sharpening coaxial line is described, with particular application to the SLC Polarized Light Source.

### 1. Introduction

The SLAC Linear Collider (SLC)<sup>1</sup> is now installing and commissioning hardware to provide polarized electron beams for high energy particle physics research.<sup>2</sup> The classical photoelectric effect can be used to produce polarized bunches of electrons from a GaAs photocathode when the incident light is circularly polarized. The Polarized Light Source (PLS) consists of a high power dye laser and the necessary optics to shape and transport the light beam to the photocathode in the electron gun. The system timing requirements on the light pulse cannot be met directly by the laser and the beam must be optically chopped by means of fast electro-optical modulators. Figure 1 outlines the principal features and specifications of the Laser Pulse Chopper (LPC) which performs this function.

---

\* Work supported by Department of Energy contract DE-AC03-76SF00515.

The laser beam passes first through a linear polarizer followed by two Pockels cells<sup>3</sup> and a final polarizer, or analyzer, aligned at 90° to the initial polarizer. A Pockels cell is a voltage-variable birefringent crystal which responds to a voltage across the crystal electrodes by rotating the vector of linearly polarized light. The cells are mechanically tuned at zero volts for maximum beam extinction (zero retardation) and either of the cells can independently rotate the beam polarization by the application of high voltage. Two cells are needed to provide the double pulse structure required by the SLC as shown in Figure 1. (The third cell shown in the figure is a voltage-variable quarter wave plate used to transform the beam polarization from linear to circular. This cell is not part of the LPC.) When voltage is applied to a Pockels cell in this arrangement the light which is transmitted will have an intensity related to the applied voltage by the expression

$$I = I_0 \sin^2 \left( \frac{\pi}{2} \frac{V_p}{V_\pi} \right) , \quad (1)$$

where  $V_p$  is the peak pulse voltage and  $V_\pi$  is 2300 V for the selected Pockels cell at the operating wavelength of 750 nm. Referring to Figure 1 the LPC requires a voltage pulse into 50  $\Omega$  of 2300 V peak with a FWHM of 2.5 ns and a full base width less than 3.0 ns at 2% of peak level. This pulse must be stable in amplitude to better than 4.5% and have less than 15 ps (sigma) timing jitter. In addition there is a tight requirement on pre-pulse leakage and after-pulse ringing on time scales up to 300 ns before and after the pulse. Lastly, the LPC is required to operate unattended at 120 Hz for 500 hours or more.

Most fast high voltage pulse generators use gas-filled switch tubes to achieve short risetimes. Krytrons, thyratrons and triggered spark gaps are commonly used to achieve nanosecond risetimes to voltages well in excess of those required by the PLS. These devices are all subject to leading edge timing jitter at the nanosecond level and have either short lifetime or limited repetition rates. Solid-state devices, on the other hand, achieve kilohertz rep rates but at inadequate risetimes. Moreover their jitter performance, though superior to switch tubes, is still inadequate to meet the SLC specification.

The SLC produces unpolarized beams which meet the above timing specifications using a pulsed thermionic diode gun driven by a unique hybrid generator consisting of low voltage avalanche transistors with excellent jitter and adequate speed, coupled to a two-stage planar triode amplifier.<sup>4,5</sup> This generator produces 300 V peak

pulses which meet all of the PLS specifications except for peak voltage. By suitable modifications the generator has been made capable of producing pulses up to 5000 V though not to the timing parameters required for the PLS. For a variety of reasons the generator as designed cannot achieve the 2000 V/ns needed by the LPC. However, since this technology existed an effort was made to speed up the pulse produced by this device. It should be mentioned that other designs using planar triodes have been described which do appear to have sufficient slew rate for the purposes of the LPC.<sup>6</sup> Those designs were not available when the work reported here was being done.

## 2. Magnetic Compression

The technique of magnetic pulse compression, also called pulse sharpening, has been known and successfully applied for some time.<sup>7-11</sup> A typical application consists of one or more stages of discrete lumped LC lowpass filters forming a delay line as shown in Figure 2. The inductor is designed to magnetically saturate sometime during the leading edge of the drive pulse. The network then "switches" from longer to shorter delay time, which can be made to speed up the leading edge of the transmitted pulse. The later portions of the edge travel faster and "catch up" to the earlier portions somewhat as a water wave steepens in running over a sloping sea bottom. Cascading stages can yield remarkable results with nanosecond risetimes to 50,000 V being reported.<sup>8,11</sup> Theoretical limits on risetimes of 40 ps per inductance element have been calculated based on the spin relaxation rates in ideal ferrites. When stray reactances in coupled circuits are taken into account this risetime degrades to nanoseconds.<sup>9</sup> A related design is the ferrite-loaded coaxial line,<sup>10,11</sup> also reported to achieve significant pulse leading edge sharpening. This geometry is basically just a distributed circuit version of the lumped design and operates by the same principles.

We have applied these techniques in speeding up the high voltage pulse used at the SLC PLS and have achieved performance somewhat better than previously reported. A major difference in our application is the fact that we do not have the typically 1000 A which were used in the applications above but are limited to less than 100 A. Since the current gain in planar triodes declines rapidly with age it would be desirable to be able to work down to 50 A (2500 V into 50  $\Omega$ ). For this reason the standard magnetic materials are precluded because they either exhibit high coercive force (requiring high magnetizing currents) or else have low resistivity with resultant high frequency loss. We found that a type of ferrite composition not normally used

at the highest frequencies actually has the best combination of properties for this application. This material,<sup>12</sup> summarized in Table 1, combines low  $H_c$ , relatively high  $\rho_v$ , high  $\mu_{max}$  and most significantly a large difference between  $B_s$  and  $B_r$ , i.e. it is not a square-loop material. Square-loop, or magnetically hard, core materials are normally selected for magnetic amplifier and compressor applications because they have the largest gains due to their high maximum permeability  $\mu_{max}$ . The change in inductance, and therefore wave speed, through a network depends on the change in  $\mu$ . Square-loop materials can have  $\mu_{max}$  (relative) as high as a million. But all such materials have low resistivities and are unusable at nanosecond speeds. Moreover, because their hysteresis loops are flat-topped, or square, they require reset currents opposite to the pulse current to reset the core to a suitable point between pulses, so that the maximum range of  $\mu$  can be utilized (see Figure 3). At the very highest frequencies the electrical connections required for the reset circuit impose unavoidable stray reactances which degrade the output pulse waveform. It was found that by eliminating the reset circuit much smoother pulses resulted and that soft magnetic materials with  $B_r$  substantially lower than  $B_s$  have enough range in  $\mu$  to provide pulse sharpening without resetting the loop externally.

### 3. Design of a Pulse Sharpener

To eliminate pre-pulse due to stray coupling across the network the pulse sharpener was made in a coaxial line geometry. After-pulse ringing was eliminated by close-coupling the line to wideband high voltage connectors<sup>13</sup> without additional circuit connections as described above. The unit inductance  $L_i$  was formed by a single ferrite bead over a 0.025" diameter wire and the unit capacitance  $C_i$  by a copper tubing spacer of appropriate length (Figure 4) with a low-loss dielectric layer of polyolefin tubing<sup>14</sup> maintaining the centering and voltage standoff within the outer coaxial tube. The unit cell dimensions were chosen to be  $\ll 1/8$  wavelength of the highest frequency present in the sharpened output pulse to avoid ringing. This allowed the use of a simple lumped circuit analysis in the design.<sup>15</sup>

A detailed analysis of an  $N$ -element cascaded network would require elaborate numerical modelling, since the ferrite becomes increasingly lossy as the frequency content of the pulse goes up. Above 100 MHz the imaginary component  $\mu''$  exceeds the real permeability  $\mu'$  but no detailed data exist for these commercial ferrites.<sup>16</sup> And even if one can adequately model a single section, at any given instant each

of the  $N$  sections will be in a different state. For a large number of sections the simulation would most likely fail to approximate the performance of the real line. Another problem facing an analytical design approach is that, by the nature of its action, the line presents a varying impedance both to the pulse generator, as a load, and to the driven line, as a source. It would seem impossible to make a saturating line match both a fixed impedance source and load without severe reflections and loss.

However, if the saturating line is located electrically close to the generator then the source mismatch is inconsequential and only the load must be matched. The anode of an ideal vacuum triode is approximately a current source into low impedance loads since the plate impedance is in the kilohm range as long as the anode voltage is above saturation.<sup>17</sup> For frequencies close to the gain-bandwidth cutoff and currents close to saturation the triode departs from the ideal behavior and the individual tube curves must be used for design. Two parallel Eimac<sup>18</sup> Y-690 planar triodes have a minimum plate impedance of  $150 \Omega/2$  or  $75 \Omega$ . The maximum output pulse amplitude into  $50 \Omega$  is then only  $0.4 V_p$  and is actually lower due to saturation nonlinearity.

The characteristic impedance of an ideal lossless coaxial line of inner radius  $a$  and outer radius  $b$  is ( $\mu_r$  and  $\epsilon_r$  are relative quantities)

$$Z_0 = 60 \sqrt{\frac{\mu_r}{\epsilon_r}} \ln \frac{b}{a} \quad (2)$$

If the compressor line impedance goes to  $50 \Omega$  as  $\mu_r$  goes to 1 then the load can be matched without loss. In this case the maximum impedance presented by the line to the source will occur when the ferrite cores are at  $\mu_{max}$  which for the Type H material is as high as 4300. Then the maximum line impedance will be

$$Z_{max} = 50 \sqrt{4300} \simeq 3300 \Omega \quad (3)$$

This is greater than the plate impedance over most of the voltage swing so the tube acts much like a voltage source. As the line is driven into magnetic saturation its impedance drops and the tube gradually approximates a current source. Lastly, at saturation the compressor line is designed to reach  $50 \Omega$  and can drive a cable of any length without mismatch. The residual losses in the line are those due to conductor skin effect and dielectric absorption in the ferrite and the polyolefin. In practice, we have achieved less than 10% loss into long cables with number of sections  $N$  as high as 60.

So with these considerations it is relatively easy to design a multi-stage magnetic pulse compression line using simple lumped element transmission line formulae. The characteristic impedance of the line goes to

$$Z_0 = \sqrt{\frac{L_i}{C_i}} = \frac{60}{\sqrt{\epsilon_r}} \ln \frac{b}{a} \quad (4)$$

when  $\mu_r \rightarrow 1$ . The unit capacitance is, in practical units

$$C_i = 1016 \frac{\sqrt{\epsilon_r}}{Z_0} [pF/ft] = 84.67 \frac{\sqrt{\epsilon_r}}{Z_0} [pF/in] \quad (5)$$

from which follows the unit inductance

$$L_i = Z_0^2 C_i [H/unit \text{ length of } C_i] = 5.08 \ln \frac{b}{a} [nH/in] \quad (6)$$

And the saturated TEM wave speed in the line is

$$c' = \frac{c}{\sqrt{\mu_r \epsilon_r}} \rightarrow \frac{c}{\sqrt{\epsilon_r}} \quad (7)$$

These formulae neglect losses which are in fact on the order of 10% largely due to dielectric absorption in the ferrite. The only quantities needed for the design are the drive pulse leading edge risetime  $\tau$  and the effective dielectric constant of the composite line which depends on the dimensions of the capacitance section,  $\epsilon_r$  for the polyolefin tubing, for the ferrite beads themselves, and using  $\epsilon_r = 1$  for any air space in the design.

Using the parameters listed in Appendix A an  $N = 58$  line was made and measured to have a capacitance of 140 pF or 3.9 pF/in. From a geometrical inductance of 4.0 nH/section or 6.5 nH/in this represents an actual  $Z_0 = 41 \Omega$ . Ideal TEM wave speeds are 0.72  $c$  and 0.89  $c$  for the coaxial and bead sections, respectively. Therefore the transit time delay is 59 ps and 12 ps, respectively, and a 58 section line has a fully saturated transit time  $t = 4.1$  ns. Ideally a saturating line will produce a pulse with zero risetime. Again, though this is unrealistic, it simplifies the calculation to assume the limiting case. For an ideal speed-up of a pulse leading edge with a long risetime there is a simple relationship between initial and final transit time through the line (denoting transit time  $t$  and risetime  $\tau$ )

$$t_i - t_f = \tau \quad (8)$$

Using  $\tau = 5$  ns for the risetime of the planar triode amplifier pulse and  $t = l/c'$  it is apparent that the ideal design length of the line is

$$l = \frac{c\tau}{\sqrt{\epsilon_r}} \left( \frac{1}{\sqrt{\mu_i} - \sqrt{\mu_f}} \right) \quad (9)$$

If  $\mu_i = 4300$  and  $\mu_f = 1$  this formula results in a very short design length. But, in fact, the line does not saturate due to finite current so  $\mu_f$  is larger than 1 but unknown, and since only the minor  $B$ - $H$  loop from  $B_r$  to  $\sim B_s$  is being traversed  $\mu_i$  is not as high as  $\mu_{max}$  but is also unknown (see Figure 5). So to determine the optimum design length we tested the response of various length lines and found that there was an optimum trade-off between increasing risetime and decreasing amplitude for number of beads  $N \sim 50$ -60. The results of this study are shown in Figure 5.

#### 4. Performance of the Pulse Sharpener

Figure 7 shows an oscilloscope<sup>23</sup> trace of both the generator drive pulse and the output of the compressor line. A 5 ns risetime has been shortened to just over 1 ns which is adequate for the SLC PLS. Note the absence of pre-pulse feedthrough and ringing. Additional pulse-forming is required to filter out from this sharpened pulse the narrow pulse used by SLC. A simple RC highpass filter is sufficient to shape the pulse as shown in Figure 8.

Since low timing jitter is essential in the SLC the jitter contribution of this line was extensively studied using a wideband sampling oscilloscope with waveform analysis and histogramming capability.<sup>23</sup> On both short (10 seconds) and medium (several minutes) timescales the RMS jitter was less than 10 ps, and on timescales of hours the slow drift was within 30 ps. The slow drift is readily correctable by control system feedback to the trigger pulse timing and is probably due to thermal drift in the avalanche transistor  $V_{BE}$ . The short-term jitter is well below the SLC requirement and is a major achievement in a high voltage pulse this short. It is worth pointing out that these results show that the magnetic pulse compression technique does not impose an inherent penalty in timing jitter, as is widely thought. Careful magnetic shielding and vibrational decoupling of the line prevent stray magnetic fields from biasing the operating point. The small range in  $\mu$  over which the ferrite changes undoubtedly contributes as well. A larger range of permeability results in an increased sensitivity to small changes in drive signal amplitude with the result that amplitude

noise translates into timing jitter. By using only a small minor  $B-H$  loop the noise sensitivity is reduced.

## 5. Conclusion

The design of magnetic compression pulse sharpening coaxial lines is relatively simple and the devices exhibit exceptional short- and long-term stability. With the use of simple lumped-element design formulae it is possible to adapt this technique to a number of requirements calling for fast-rising high voltage pulses with low timing jitter.

NOTE ADDED IN PROOF: Further research with ferrite-loaded coaxial lines utilizing high-purity quartz in place of the polyolefin dielectric has yielded preliminary results indicating that this construction may perform significantly better than that which is described here. This work is still in progress.

## Appendix A: Design Parameters for the SLC LPC Compression Line

The following design parameters were chosen for the SLC PLS high voltage pulse compression line (see Figure 9): unit length  $l_i = 0.625''$  divided into  $l_b = 0.125''$  for the ferrite bead and  $l_c = 0.500''$  for the capacitance spacer; coaxial dimensions  $b = 0.124''$  outer diameter, and  $a = 0.075''$  inner diameter, determined by the size of the available beads and standard thin wall tubing. The beads and spacer sections were strung on a  $0.025''$  diameter drawn copper wire with solder joints linking the spacers to the wire at each junction. Care was taken in assembly to leave smooth continuous joints devoid of solder points or flux residues which would act as electric field stress concentrations and cause breakdown. Since thin-wall copper tubing with the correct OD was not available with ID =  $0.025''$ , inner support tubes of high temperature fluoropolymer heat shrink were used to keep the capacitance spacers concentric to the wire. The same shrink tubing, in a larger size, was used to center the composite line within the outer coax tube to provide an air gap for additional voltage standoff. Sections of tubing shorter than the beads ( $\sim 0.06''$  long) were shrunk over the ferrite sections only, since this material has significant dielectric absorption and would degrade the signal propagation if used in the capacitance sections. The overall dielectric consisted of  $\sim 0.015''$  low-loss polyolefin with  $\epsilon_r = 2.55$  and  $\tan \delta = 0.0003$  at  $500 \text{ MHz}$ <sup>19</sup> and  $0.010''$  air space with nearly ideal transmission properties. The low frequency dielectric constant of the ferrite was determined empirically by stringing a test line consisting only of beads and polyolefin and measuring its capacitance. The effective  $\epsilon_r$  for the bead sections was found to be 4.9. Applying Eqs. (4) and (5) the capacitance of the bead sections was  $\sim 0.4 \text{ pF/bead}$ . By the same calculation the capacitance sections were  $\sim 2.7 \text{ pF/spacer}$  for a total  $C_i \sim 3.1 \text{ pF}$ . The unit inductances can be calculated from geometrical principles<sup>20</sup> or from Eqs. (2), (5) and (6). The bead section at full saturation has  $\sim 2.8 \text{ nH}$  and the spacer  $\sim 1.3 \text{ nH}$ . The overall saturated impedance of the line then is  $\sim 36 \Omega$ , in fair agreement with the measured properties of the finished line (Section 3). This final impedance must be designed to be less than  $50 \Omega$  for the practical reason that the ferrite really does not get all the way to  $\mu_r = 1$  due to insufficient current. The factor of 1.3 in the design compensates for this and the measured losses show that the  $50 \Omega$  match is fairly well achieved.

## References

1. *SLC Design Handbook*, Stanford Linear Accelerator Center, Stanford University, 1984.
2. Blockus, D. *et al.*, *Proposal for Polarization at the SLC*, SLAC-PROPOSAL-SLC-UPGRADE-01, Stanford Linear Accelerator, Stanford University, 1986.
3. *Model 1072 Lasermetrics*, Electro-Optics Division, NJ.
4. Browne, M. J. *et al.*, *A Multi-Channel Pulser for the SLC Thermionic Electron Source*, SLAC-PUB-3546, Stanford Linear Accelerator, Stanford University, 1985.
5. Clendenin, J.E. *et al.*, *Timing Stabilization for the SLC Electron Source*, SLAC-PUB-4231, Stanford Linear Accelerator, Stanford University, 1987.
6. Booth, R. *et al.*, *Ultrafast High Voltage Pulse Generation Using Planar Triodes*, preliminary report, Lawrence Livermore National Laboratory, no date. Contact author for further information.
7. Kirbie, H. C., *Proceedings of the Switched Power Workshop*, Shelter Island, New York, October 16-21, 1988, ed. Richard C. Fernow, Brookhaven National Laboratory publ. BNL 52211, p. 219 ff. and references therein.
8. Birx, D. L., *et al.*, *IEEE Trans. Nucl. Sci. NS-32 (5)*, October 1985, p. 2743 ff.
9. Katayev, I. G. *et al.*, *Izvestiya vuzov SSSR—Radioelektronika*, Vol. 17, No. 12, 1974, p. 40 ff., translated in SLAC TRANS-0229, Stanford Linear Accelerator Center, 1989.
10. Weiner, M. *et al.*, *IEEE Trans. Magnetics MAG-17 (4)*, July 1981, p. 472 ff.
11. Seddon, N., *et al.*, *Rev. Sci. Instr.* 59 (11), November 1988, p. 2497 ff. and references therein.
12. *Type H ferrite*, National Magnetics Group, Inc., Newark, NJ.
13. Amphenol type HN, Amphenol RF/Microwave Operations, Danbury CT.
14. Raychem *RNF 100*, Raychem Inc., Menlo Park CA.
15. Ramo, S. *et al.*, *Fields and Waves in Communication Electronics*, 2nd ed., John Wiley & Sons, 1984, or any general reference on transmission line theory.
16. Representative behavior of various research formulations of ferrites can be found in: Gurevich, A., *Ferrites at Microwave Frequencies*, trans. A. Tybulewicz, Consultants Bureau Enterprises, Inc., New York, 1963; Clarricoats, P., *Microwave Ferrites*, John Wiley & Sons, Inc., New York, 1961.

17. Spangenberg, K., *Fundamentals of Electron Devices*, McGraw Hill, New York, 1957.
18. Varian Eimac, Salt Lake City, UT.
19. These values differ from those for pure polyethylene due to proprietary additives used to make the tubing heat shrinkable.
20. Grover, F., *Inductance Calculations*, Van Nostrand, Inc., New York, 1946.
21. Typical high frequency soft ferrite formulation.
22. Typical square-loop material used in magnetic switching applications. "Metglas" is a registered trademark of Allied Signal Corp., Parsippany, NJ.
23. Hewlett Packard 54121T 12.4 GHz digitizing sampling oscilloscope.

Table 1.  
Comparison of national type H vs. type M<sub>3</sub><sup>20</sup> and Metglas 2714A<sup>21</sup>.

Parameter	Unit	Type H	Type M <sub>3</sub>	Metglas 2714A
$\mu_{max}$	(rel. $\mu_0$ )	4300	50	1,000,000
$B_s$	Gauss	3400	2700	5200
$B_r$	Gauss	1500	1500	5200
$H_c$	Oersted	0.18	20.0	0.001
$\rho_v$	$\Omega$ -cm	$10^5$	$10^8$	$10^{-4}$

FIGURE 1: Principle Features of the SLC PLS

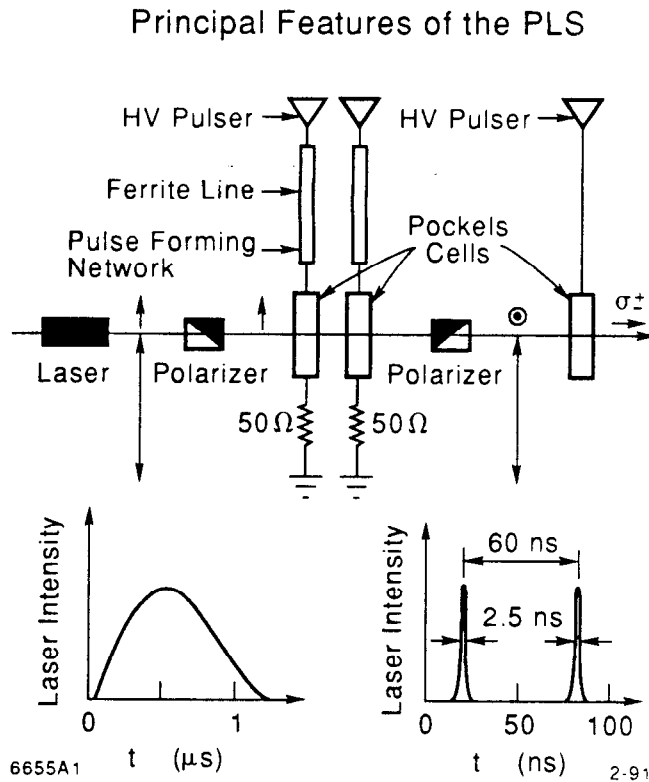


**FIGURE 2:** Saturating *LC* Lowpass Delay Line.

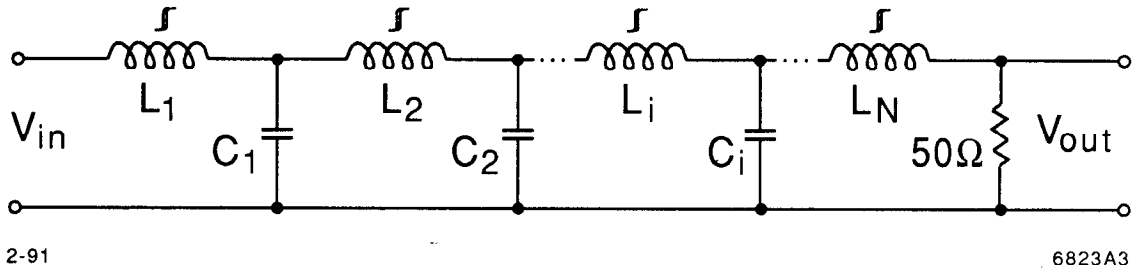


**FIGURE 3:** *B-H* Curves of Hard vs. Soft Magnetic Materials.

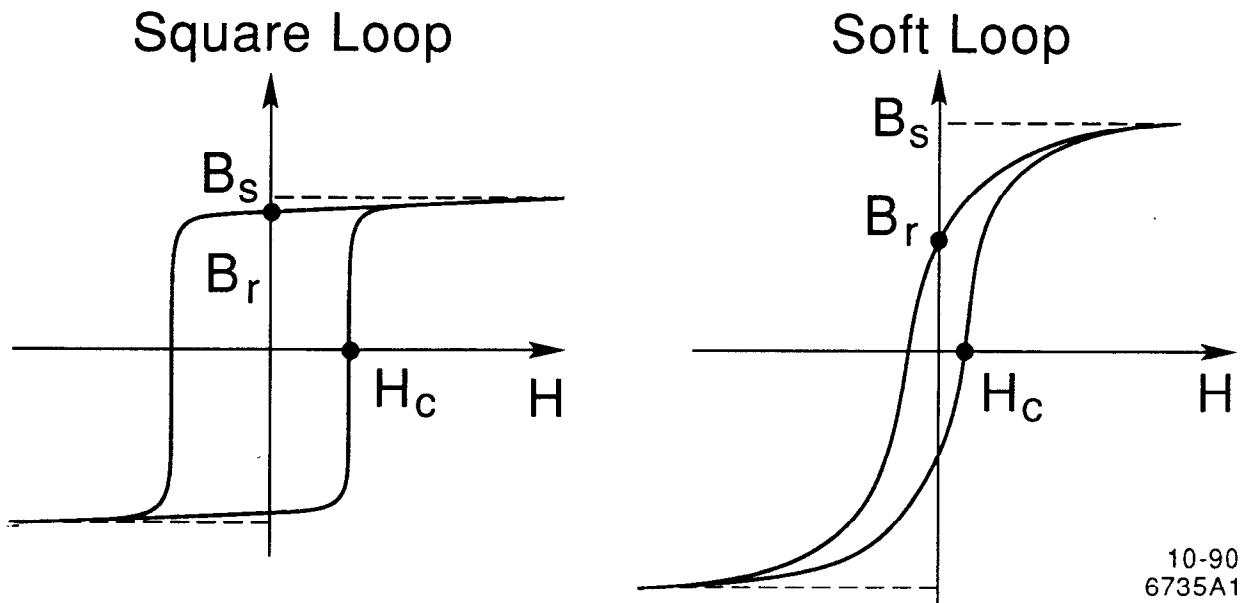
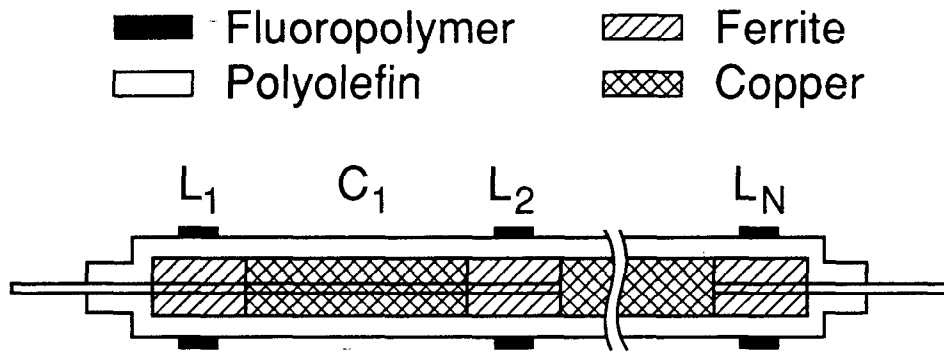


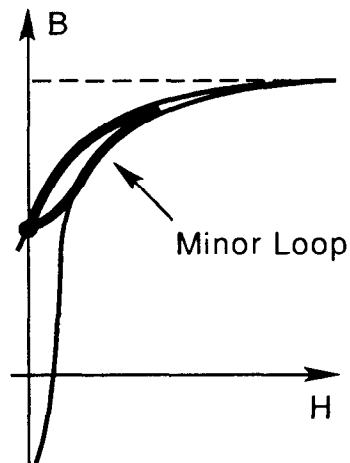
**FIGURE 4:** Layout of Components of Magnetic Pulse Compression Line.



2-91

6823A9

**FIGURE 5:**  $B$ - $H$  Curve Showing Minor Loop  $B_r$  to  $\sim B_{max}$



12-90

6735A2

**FIGURE 6:** Number of beads ( $N$ ) vs. Ristime 10-90% ( $t_r$ ).

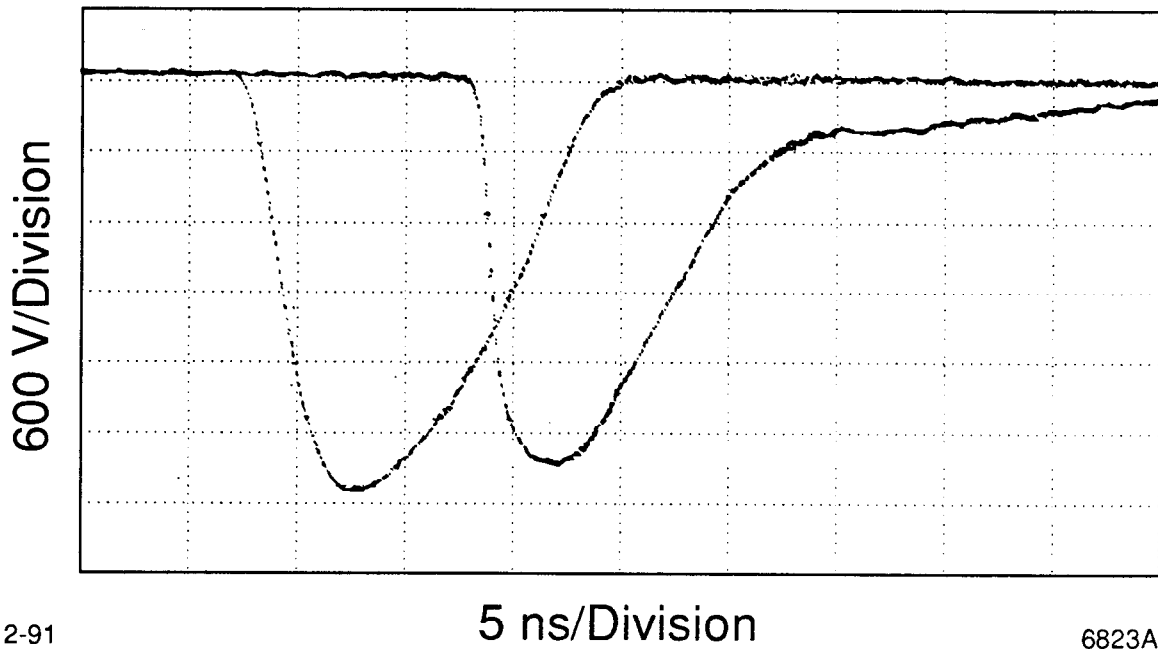
---

N	65	60	55	50	45	40
$t_r$	1.48	1.42	1.38	1.50	1.54	1.74

2-91

6823A7

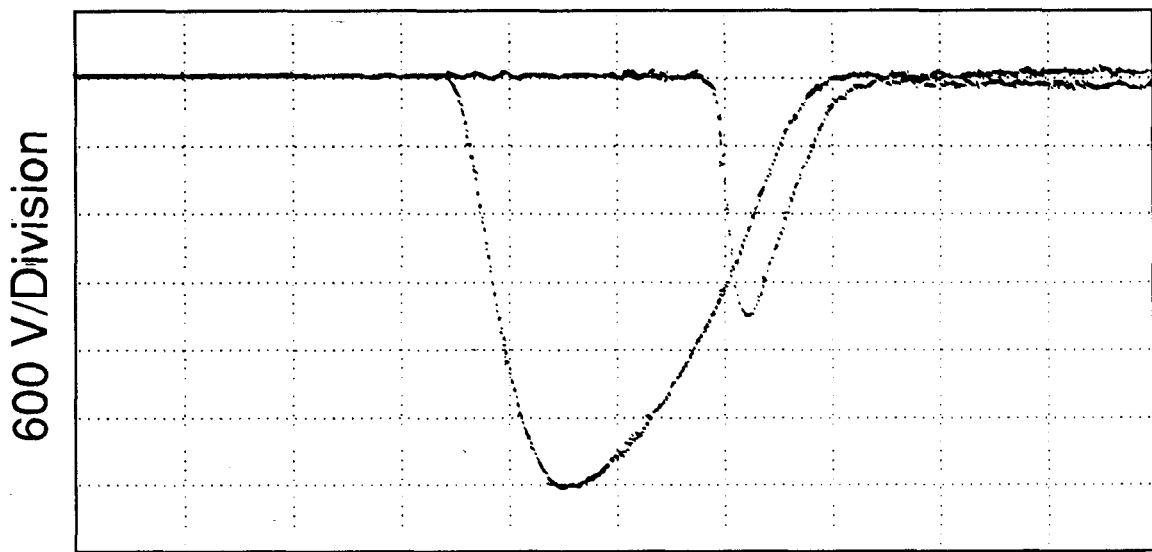
**FIGURE 7:** Direct Generator Output Pulse vs. Compressor Output.



2-91

6823A1

**FIGURE 8:** Generator Output Pulse vs. Highpass Filter Output.

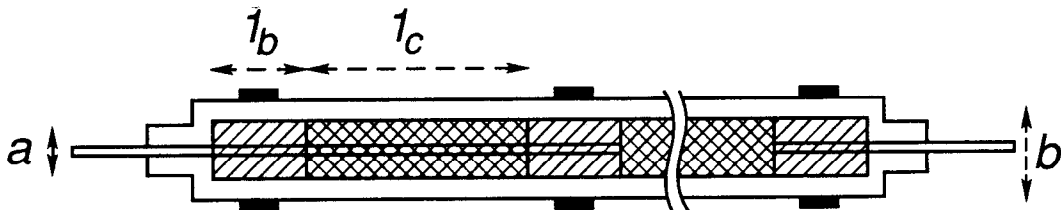


2-91

5 ns/Division

6823A2

**FIGURE 9:** Construction of the LPC Magnetic Compression Line



2-91

6823A8

#### APPENDIX A: Design Parameters for the SLC LPC Compression Line

The following design parameters were chosen for the SLC PLS high voltage pulse compression-line (refer to Figure 9): unit length  $l_i = 0.625''$  divided into  $l_b = 0.125''$  for the ferrite bead and  $l_c = 0.500''$  for the capacitance spacer; coaxial dimensions  $b = 0.124''$  outer diameter, and  $a = 0.075''$  inner diameter, determined by the size of the available beads and standard thin wall tubing. The beads and spacer sections were strung on a  $0.025''$  diameter drawn copper wire with solder joints linking the spacers to the wire at each junction. Care was taken in assembly to leave smooth continuous joints devoid of solder points or flux residues which would act as electric field stress concentrations and cause breakdown. Since thin-wall copper tubing with the correct OD was not available with  $ID = 0.025''$ , inner support tubes of high temperature fluoropolymer heat shrink were used to keep the capacitance spacers concentric to the wire. The same shrink tubing, in a larger size, was used to center the composite line within the outer coax tube to provide an air gap for additional voltage standoff. Sections of tubing shorter than the beads ( $\sim 0.06''$  long) were shrunk over the ferrite sections only, since this material has significant dielectric absorption and would degrade the signal propagation if used in the capacitance sections. The overall dielectric consisted of  $\sim 0.015''$  low-loss polyolefin with  $\epsilon_r = 2.55$  and  $\tan \delta = .0003$  at  $500 \text{ MHz}$ <sup>19</sup> and  $0.010''$  air space with nearly ideal transmission properties. The low frequency dielectric constant

of the ferrite was determined empirically by stringing a test line consisting only of beads and polyolefin and measuring its capacitance. The effective  $\epsilon_r$  for the bead sections was found to be 4.9. Applying eqns. 4 and 5 the capacitance of the bead sections was  $\sim 0.4$  pF/bead. By the same calculation the capacitance sections were  $\sim 2.7$  pF/spacer for a total  $C_i \sim 3.1$  pF. The unit inductances can be calculated from geometrical principles<sup>20</sup> or from eqns. 2, 5 and 6. The bead section at full saturation has  $\sim 2.8$  nH and the spacer  $\sim 1.3$  nH. The overall saturated impedance of the line then is  $\sim 36 \Omega$ , in fair agreement with the measured properties of the finished line (Section 3). This final impedance must be designed to be less than  $50 \Omega$  for the practical reason that the ferrite really does not get all the way to  $\mu_r = 1$  due to insufficient current. The factor of 1.3 in the design compensates for this and the measured losses show that the  $50 \Omega$  match is fairly well achieved.

## REFERENCES:

---

- 1) *SLC Design Handbook*, Stanford Linear Accelerator Center, Stanford University, 1984.
- 2) Blockus, D. *et al.*, *Proposal for Polarization at the SLC*, SLAC-PROPOSAL-SLC-UPGRADE-01, Stanford Linear Accelerator, Stanford University, 1986.
- 3) *Model 1072* Lasermetrics, Electro-Optics Division, NJ.
- 4) Browne, M.J. *et al.*, *A Multi-Channel Pulser for the SLC Thermionic Electron Source*, SLAC-PUB-3546, Stanford Linear Accelerator, Stanford University, 1985.
- 5) Clendenin, J.E. *et al.*, *Timing Stabilization for the SLC Electron Source*, SLAC-PUB-4231, Stanford Linear Accelerator, Stanford University, 1987.
- 6) Booth, R. *et al.*, *Ultrafast High Voltage Pulse Generation Using Planar Triodes*, preliminary report, Lawrence Livermore National Laboratory, no date. Contact author for further information.
- 7) Kirbie, H.C., *Proceedings of the Switched Power Workshop*, Shelter Island, New York, October 16-21, 1988, ed. Richard C. Fernow, Brookhaven National Laboratory publ. BNL 52211, p. 219 ff. and references therein.
- 8) Birx, D. L., *et al.*, *IEEE Trans. Nucl. Sci. NS-32 (5)*, October 1985, p. 2743 ff.
- 9) Katayev, I. G. *et al.*, *Izvestiya vuzov SSSR—Radioelektronika*, Vol. 17, No. 12, 1974, p. 40 ff., translated in SLAC TRANS—0229, Stanford Linear Accelerator Center, 1989.
- 10) Weiner, M. *et al.*, *IEEE Trans. Magnetics MAG-17 (4)*, July 1981, p. 472 ff.
- 11) Seddon, N., *et al.*, *Rev. Sci. Instr. 59 (11)*, November 1988, p. 2497 ff. and references therein.
- 12) *Type H ferrite*, National Magnetics Group, Inc., Newark NJ.
- 13) Amphenol type *HN*, Amphenol RF/Microwave Operations, Danbury CT.
- 14) Raychem *RNF 100*, Raychem Inc., Menlo Park CA.
- 15) Ramo, S. *et al.*, *Fields and Waves in Communication Electronics*, 2nd. ed., John Wiley & Sons, 1984, or any general reference on transmission line theory.
- 16) Representative behavior of various research formulations of ferrites can be found in: Gurevich, A., *Ferrites at Microwave Frequencies*, trans. A. Tybulewicz, Consultants Bureau Enterprises, Inc., New York, 1963; Clarricoats, P., *Microwave Ferrites*, John Wiley & Sons, Inc., New York, 1961.
- 17) Spangenberg, K., *Fundamentals of Electron Devices*, McGraw Hill, New York, 1957.
- 18) Varian Eimac, Salt Lake City, UT.
- 19) These values differ from those for pure polyethylene due to proprietary additives used to make the tubing heat shrinkable.

20) Grover, F., *Inductance Calculations*, Van Nostrand, Inc., New York, 1946.

21) Typical high frequency soft ferrite formulation.

22) Typical square-loop material used in magnetic switching applications. "Metglas" is a registered trademark of Allied Signal Corp., Parsippany NJ.

23) Hewlett Packard 54121T 12.4 GHz digitizing sampling oscilloscope.